should be investigated during the aircraft design cycle, even if larger scale models with less flowfield simulation are utilized initially.

References

[1]Glasgow, E. R., Santman, D. M., and Miller, L. D., et al., "Integrated Airframe-Nozzle Performance for Designing Twin-Engine Fighters," AFFDL-TR-73-71, June 1973, Air Force Flight Dynamics Lab., Wright-Patterson Air Force Base, Ohio.

[2]Galigher, L. L., "Integrated Airframe Nozzle Performance Characteristics of a Generalized Twin-Jet, Air Superiority Fighter Aircraft Model at Mach Numbers From 0.6 to 1.6." AEDC-TR-73-125, July 1973, Arnold Engineering Development Center, Tullahoma, Tenn.

[3]Glasgow, E. R., Santman, D. M., and Miller, L. D., et al., "Experimental and Analytical Determination of Integration Airframe-Nozzle Performance," AFFDL-TR-72-101, Oct. 1972, Air Force Flight Dynamics Lab., Wright-Patterson Air Force Base, Ohio.

[4]Presz, W., "Experimental and Analytical Determination of Integrated Airframe-Nozzle Performance, Phase III Summary Report, Pratt & Whitney Aircraft Support Program," PWA-4503, July 1972, Pratt and Whitney, East Hardford, Conn.

[5]Glasgow, E. R., Divita, J. S., Everling, P. C., and Laughrey, J. A., "Analytical and Experimental Evaluation of Performance Prediction Methods Applicable to Exhaust Nozzles," AIAA Paper 71-719, Salt Lake City, Utah, 1971.

[6]Glasgow, E. R. and Santman, D. M., "Aft-End Design Techniques for Twin-Engine Fighters," *Journal of Aircraft.*, Vol., No. 1, Jan. 1974, pp. 39-44.

[7]General Dynamics/Fort Worth Division, "Supersonic Inlet Design and Airframe-Inlet Integration Program (Project Tailor-Mate)," AFFDL-TR-71-124, May 1973, Air Force Flight Dynamics Lab., Wright-Patterson Air Force Base, Ohio.

JUNE 1974 J. AIRCRAFT VOL. 11, NO. 6

Engineering Notes

ENGINEERING NOTES are short manuscripts describing new developments or important results of a preliminary nature. These Notes cannot exceed 6 manuscript pages and 3 figures; a page of text may be substituted for a figure and vice versa. After informal review by the editors, they may be published within a few months of the date of receipt. Style requirements are the same as for regular contributions (see inside back cover).

Vortex Measurements Behind a Swept Wing Transport Model

K. L. Orloff* and D. L. Ciffone†
NASA Ames Research Center, Moffett Field, Calif.

Introduction

A CONSIDERABLE amount of information documenting the structure of aircraft wake turbulence has been produced over the last several years. Quantitative detailing of the flow has, however, been primarily restricted to wings with simple near-rectangular or elliptic span loadings. The need for experimental velocity distributions from models of wings representative of today's modern transport aircraft is the rationale for the measurements being reported.

A backscatter laser Doppler velocimeter (LDV) which simultaneously senses two components of the velocity (axial and tangential), has been used to traverse and measure the velocity distributions in the near wake of a swept wing semi-span transport model in the NASA-Ames 7- by 10-foot wind tunnel.[1] This LDV instrument has previously been used to measure the velocity distributions in the wake of a rectangular airfoil.[2,3,4] The model configuration included nacelles, pylons, anti-shock bodies, and wing flaps which could be deflected 27°. Further details of this semispan wing model are available in Ref. 5.

Apparatus and Procedure

The semispan model was mounted vertically from the floor of the wind tunnel. The test Reynolds number per meter was nominally 1.24×10^6. Since the LDV system was restricted to the location of the optical window, the wing model was placed in a forward position in the test section to allow data to be obtained at the maximum aft location $x/b = 1.25$ where x is distance measured downstream from the wing tip and b is the wing span ($b/2$ = 91.5 cm.). Data were also obtained at $x/b = 0.49$, and a full study was made of the streamwise dependence of the velocity fields with changes in wing configuration.[1] At each location both the LDV measuring station and the model position were well within the test section to insure flow uniformity.

LDV scanning was performed in a direction normal to the tunnel centerline, with the upper wing surface closest to the window through which the measurements were taken. The complication of vortex movement within the test section has been overcome as a result of the spatial scanning capability of the laser velocimeter. The Doppler information was processed on two separate spectrum analyzer systems as the focal point of the velocimeter was continuously traversing the vortex. The scan automatically reversed at end limits which were preset to contain the flow area of interest. Full details on signal processing, data acquisition, and core identification are given in Refs. 1,2, and 3.

Velocity distributions are presented as fractions of free-stream velocity, U , and location Z, relative to the trailing edge ($Z = 0$), normalized by the span, b. A positive value for Z/b indicates a location on the side below the wing planform.

Results and Discussion

Typical wake vortex velocity profiles are presented in Figs. 1 and 2 for the flaps-retracted and the flaps-deployed 27° configurations, respectively. It can be seen that the repeatability of the data for different traverses is excellent, and the vortex structure can be accurately defined. The data show a slightly higher axial velocity defect for the flaps-deployed configuration, but no perceptible change in the maximum tangential velocity. While deployment of the flaps increases the total circulation [which should increase $(V_\theta/U_\infty)_{max}$], it also alters the lift distribution, moving the center of vorticity inboard along

Received December 3, 1973; revision received April 5, 1974.
Index categories: Jets, Wakes, and Viscid-Inviscid Flow Interactions; Aircraft Aerodynamics (Including Component Aerodynamics).

*Research Scientist. Member AIAA.
†Research Scientist.

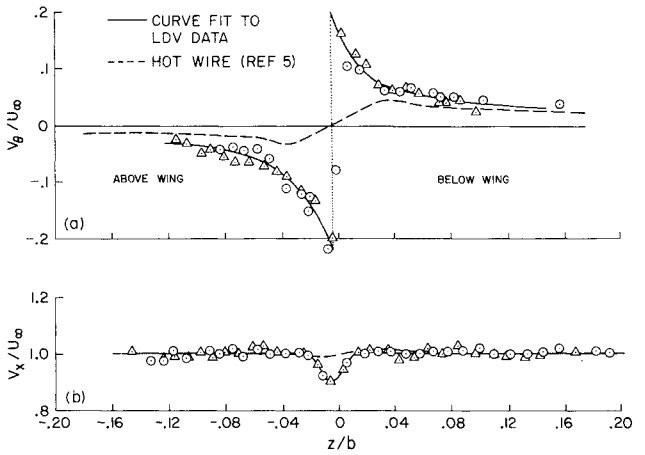

Fig. 1 Vortex velocity distributions aft of wing model for flaps-retracted configuration; $\alpha = 4.3°$, $x/b = 1.25$, $C_L = 0.20$, $U_\infty = 18.25$ m/sec; O, Δ separate traverses; a) tangential; b) axial.

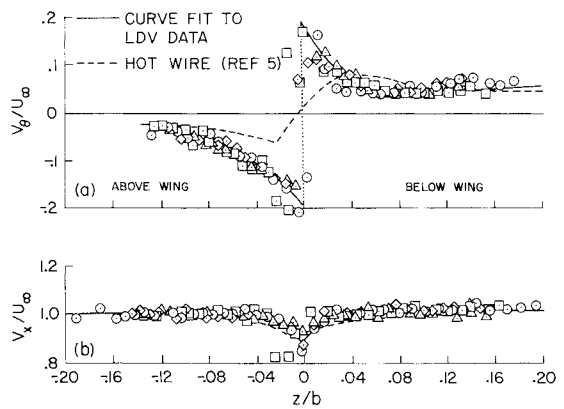

Fig. 2 Vortex velocity distributions aft of wing model for flaps-deployed configuration; $\alpha = 4.3°$, $x/b = 1.25$, $C_L = 0.39$, $U_\infty = 18.37$ m/sec; O, Δ, □, ◇ separate traverses; a) tangential; b) axial.

the span, resulting in a less concentrated vortex [which should decrease $(V_\theta/U_\infty)_{max}$]. The net effect at the particular station and test conditions shown in Figs. 1 and 2 appears as no significant change in $(V_\theta/U_\infty)_{max}$. The slight increase in the axial velocity defect is due to the increase in profile drag associated with the 27° flap deployment. The conjecture that the profile drag manifests itself as an increased velocity defect along the vortex core has been discussed at some length in other publications[3,4] with regard to a dissipator panel installed at the tip of a rectangular airfoil. The tendency of the tangential velocity to remain higher in the potential flow region below the wing as compared to above the wing is not entirely understood, although it has been observed in other vortex surveys.[3,4]

Also shown in Figs. 1 and 2 for comparative purposes are the hot-wire data of Ref. 5 obtained in the same facility and with the same model. For these measurements the hot-wire probe remained fixed, and the changing position of the vortex required that time averages be taken of the analog signal. The result was a loss of detailed structure and suppression of the actual velocities, particularly near the vortex core. This comparison again points out the need for a rapid traversal of the vortex to eliminate the problems associated with its movement within the wind tunnel. Such traversals have been accomplished with the scanning laser velocimeter used in the present experiment. A recently developed[6] instrument which utilizes a hot-wire probe at the tip of a rapidly rotating beam also overcomes the problems of vortex movement, but no results are currently available for direct comparison with the data presented herein.

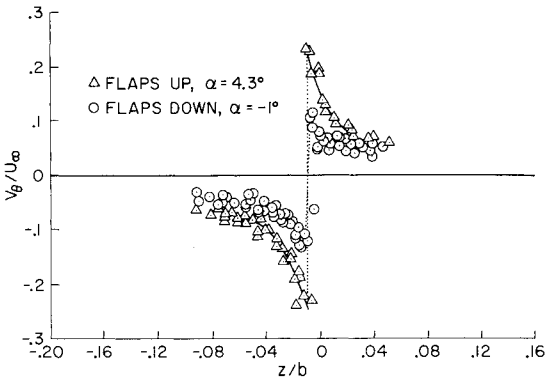

Fig. 3 Effect of span loading (flap-deflection), at constant lift coefficient, on vortex velocity distribution; $C_L = 0.20$; $x/b = 0.49$.

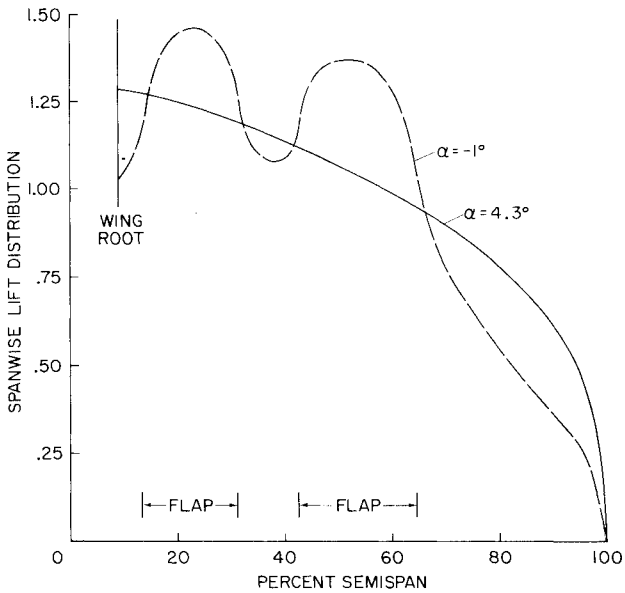

Fig. 4 Theoretical spanwise lift distribution for swept-wing planform by method of Hough.[7]

Figures 1 and 2 demonstrate the effect of flap deflection on the velocity profile for a given angle of attack. To decouple the effects of span load change and lift coefficient change, both associated with flap deployment, Fig. 3 presents the effects of span loading (flap deflection) at a constant lift coefficient. While both configurations represent a constant total lift, L, the effect of unloading the outer portion of the wing with flap deflection is to: a) considerably reduce the maximum tangential velocity; b) bring the centerlines of the two vortices closer together, thus decreasing the effective span, b', while increasing the circulation, Γ_0, of each vortex according to the relationship $L = \rho U_\infty \Gamma_0 b'$. As a result, one should expect the profiles of Fig. 3 to cross at some radius greater than $r/b = 0.08$ (the radial extent of the data). Recent, as yet unpublished, data (by these authors) from water towing experiments indicate that this may indeed be the case.

Figure 4 presents wing span loadings (normalized section lift coefficient) representative of those associated with the velocity profiles of Fig. 3. These span loadings are theoretical approximations of the lift distribution as computed by the vortex-lattice technique[7]; the influence of nacelles, pylons, and shock bodies is not considered in the computation. The inboard movement of the span loading and consequent unloading of the outer portion of the wing with flap deflection is evident. The significance of the results illustrated in Fig. 3 is to point out that a

given airplane flying at a given C_L can substantially reduce its trailing vortex upset potential by deploying its flaps and altering its flight attitude while maintaining its C_L. This concept is consistent with the theoretical prediction by Rossow[8] which indicates that additional unloading of the outer portion of the wing (relative to the inner portion) by the use of inboard flaps will produce further reductions in the maximum vortex wake velocities. These ideas and findings might be taken into consideration along with performance and noise considerations in the selection of aircraft approach L/Ds.

References

[1]Ciffone, D. L., Orloff, K. L., and Grant, G. R., "Laser Doppler Velocimeter Investigation of Trailing Vortices behind a Semi-Span Swept Wing in a Landing Configuration," TM X-62,294, Aug. 1973, NASA.

[2]Grant, G. R. and Orloff, K. L., "A Two-Color, Dual Beam Backscatter Laser Doppler Velocimeter," TM X-62,254, March 1973, NASA.

[3]Orloff, K. L. and Grant, G. R., "The Application of Laser Doppler Velocimetry to Trailing Vortex Definition and Alleviation," TM X-62,243, Feb. 1973, NASA.

[4]Orloff, K. L. and Grant, G. R., "The Application of a Scanning Laser Doppler Velocimeter to Trailing Vortex Definition and Alleviation," AIAA Paper 73-680, Palm Springs, Calif., 1973.

[5]Chigier, N. A. and Corsiglia, V. R., "Wind Tunnel Studies of Wing Wake Turbulence," *Journal of Aircraft*, Vol. 9, No. 12, Dec. 1972, p. 820.

[6]Corsiglia, V. R., Schwind, R. G., and Chigier, N. A., "Rapid Scanning, Three-Dimensional Hot-Wire Aremometer Surveys of Wing Tip Vortices," *Journal of Aircraft*, to be published.

[7]Hough, G. R., "Remarks on Vortex-Lattice Methods," *Journal of Aircraft*, Vol. 10, No. 5, May 1973, p. 314.

[8]Rossow, V. J., "On the Inviscid Rolled-up Structure of Lift-Generated Vortices," TM X-62,224, Jan. 1973, NASA.

Explicit Model Following Control Scheme Incorporating Integral Feedback

Igal Tiroshi* and Jarrell R. Elliott†

NASA Langley Research Center, Hampton, Va.

Introduction

THE type one multivariable servomechanism problem has only recently been formulated and studied in detail. Porter and Powers, in a series of letters published in Electronics Letters, and Porter[1] have described various aspects of multivariable systems which incorporate integral feedback (IFB) as a part of the control law. Young and Willems[2] reformulate the problem in what they term as a precise manner and develop "explicit and general controllability conditions for such systems." They also develop for the type one servomechanism problem a pole assignment algorithm and an algorithm based on the use of model in the performance index (MPI) optimal control theory techniques.

This Note describes the extension of the previous work to explicit model following systems for the case where IFB is incorporated into both the model and the plant dynamics. In this formulation optimal feedback control gains for the model with integral feedback are first calculated. Then the explicit model following problem, with integral feedback in the plant, is posed and solved through the use of optimal control theory.[3] (This form of model following has been called a passive adaptive scheme.[4]) As a result of this formulation of the problem, the properties of type one servomechanism systems are embodied in both the model and plant response. These and other properties of the present formulation of the problem will be discussed later. Another important feature which should be noted in the sequel is that the overall system becomes a command augmentation system.

Presented as Paper 73-862 at the AIAA Guidance and Control Conference, Key Biscayne, Fla., August 20–22, 1973; submitted August 27, 1973; revision received January 7, 1974.

Index category: Aircraft Handling, Stability, and Control.

*National Research Council Associate.

†Head, Dynamic Analysis Section. Member AIAA.

Problem Formulation

Model

$$\dot{x}_m = A_m x_m + B_m u_m + d_m \tag{1}$$

$$y_m = C_m x_m$$

Plant

$$\dot{x}_p = A_p x_p + B_p u_p + d_p \tag{2}$$

$$y_p = C_p x_p$$

x, u, y are n, r, and q vectors, respectively. A, B, and C are compatible matrices. Furthermore, C is of a special form; it is a qxn output matrix consisting of zero row elements except for one unity element in each row. Thus, C is a "selection matrix" which selects those elements of x which are to incorporate IFB and which, as will become evident, are those variables for which command control is desired. d_m and d_p are n element model and plant constant bias vectors, respectively.

Integral feedback (IFB) may be incorporated (using model Eqs. (1) to illustrate this) by defining

$$\dot{z}_m \triangleq y_r - y_m = y_r - C_m x_m \tag{3}$$

and augmenting the $\dot{x}_m$ equation with this equation. y_r is an external reference or input signal. Then defining

$$\hat{x}_m{}^T \triangleq [\, x_m{}^T \mid z_m{}^T \,]$$

The open-loop model dynamics are

$$\dot{\hat{x}}_m = \left[\begin{array}{c|c} A_m & O \\ \hline -C_m & O \end{array}\right] \hat{x}_m + \left[\begin{array}{c} B_m \\ \hline O \end{array}\right] u_m + \left[\begin{array}{c} d_m \\ \hline y_r \end{array}\right] \tag{4}$$

Infinite time optimal linear regulator theory, with performance index

$$PI_m = \int_0^\infty (\,||\hat{x}_m||_{Q_1} + ||u_m||_{R_1})\, dl$$

may be applied to obtain the gain matrices in the control law

$$u_m = -K_{PD_m} x_m - K_{I_m} z_m \tag{5}$$

Q_1 and R_1 are chosen such that "good" transient response, such as that required by satisfactory aircraft handling qualities specifications, is realized for the closed-loop model dynamics

$$\dot{\hat{x}}_m = \left[\begin{array}{c|c} A_m - B_m K_{PD_m} & -B_m K_{I_m} \\ \hline -C_m & O \end{array}\right] \hat{x}_m + \left[\begin{array}{c} d_m \\ \hline y_r \end{array}\right] \tag{6}$$

References 2 and 3 prove that the above is possible provided that (A,B) is a controllable pair and that the rank of $CA^{-1}B$ is q.

Figure 1a shows the block diagram for the closed-loop model with IFB which has the properties of 1) zero steady-steady error, 2) steady-state decoupling, 3) "good" transient response, and 4) immunity to constant bias error, d_m.